



Research Article

ISSN : 0975-7384
CODEN(USA) : JCPRC5

Design of terahertz absorbers based on metamaterial

Zhang-jing Wang* and Jiang-jiang Li

University of Electronic Science and Technology of China, Chengdu, China

ABSTRACT

We present the design of single, dual and triple resonant THz absorber based on metamaterial. The single band absorber is composed of simple ring array and the dual band absorber is the unlimited cycle array of two concentric rings. The triple absorber is produced by a ring and two square split ring with different size. Simulation results show that the three proposed designs can perform strong absorption peaks more than 90% at fundamental resonant frequencies, which show the potential of metamaterial in controlling terahertz radiation. The absorbers are uncomplicated, well-separated and strong-absorbed, which is beneficial for the design of terahertz devices.

Keywords: Metamaterial, THz wave, absorber, electric field coupling resonate.

INTRODUCTION

In recent years, there has been increasing research in metamaterial [1-5] that has specific electromagnetic responses which can not be realized in nature, such as left-handed materials [6-7], photonic crystals and super magnetic materials. Recently, it has been found that metamaterials have special advantage in the terahertz (THz) band, a band between 0.3 THz to 10 THz, where most materials in nature have been proven to exhibit weak electric and magnetic responses. Owing to good controlling of metamaterial in the terahertz (THz) band, some functional THz devices were successfully demonstrated, such as switches [8-10], absorbers [11-15], filters [16-18] and modulators [19].

Among different structures studied in the past, terahertz single-band and dual-band absorbers have already been fabricated and experimentally proved. In text [11], a symmetrical structure is proposed to produce a single band which can be adjusted by controlling dielectric layer thicknesses at 4.1, 4.2, and 4.5 THz with absorption strength of 98%, 95%, and 88%, respectively. In text [13], a dual-band metamaterial absorber was simulated and measured, which shows the absorber has two distinct and strong absorption points near 0.45 and 0.92 THz. In text [14], a kind of triple-resonant metamaterial based on asymmetric split-ring resonator (SRR) was researched, which realized three transmission minima of 23%, 25%, 42% at 0.38, 0.58, and 0.74 THz, respectively. The design and the fabrication of multi-resonant metamaterials are potentially useful in the multiple band-pass or band-stop THz devices. However, in THz regime, only a few papers present study on the multi-resonance (≥ 3), and most papers concentrated on two-resonance structure. In this letter, we have proposed three designs of single, dual and triple-resonant THz absorber based on metamaterial. Compared to earlier proposed split ring resonator (SRR) structures, the three proposed absorbers realize a good performance that the transmission minima is all below 10% and the corresponding frequency is below 0.5 THz, which are more likely to be used in the current technology condition. Besides, the resonant frequency of the proposed structures can also be regulated by changing the resonant structure size as different needs. The proposed terahertz absorbers have such good properties as strong absorption and simple structure. It may be useful to the realization of low loss 2-D planar MTM for multifunctional applications.

EXPERIMENTAL SECTION

1. DESIGN OF SINGLE RESONANT METAMATERIAL ABSORBER

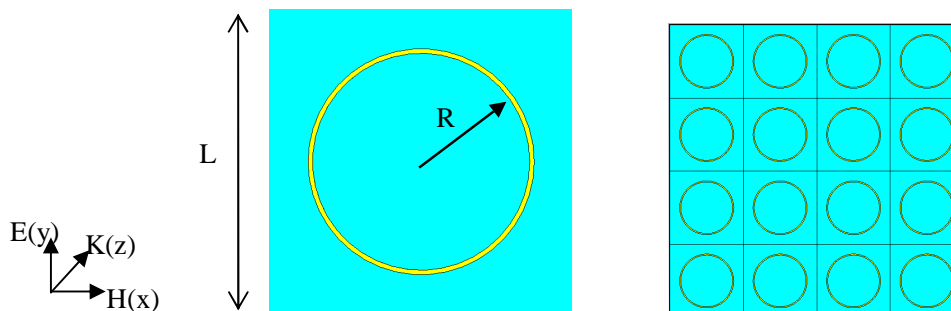


Figure 1. (a) Structural parameters of the SRR unit cell, $P=125\ \mu\text{m}$, $P_1=90\ \mu\text{m}$, $g=8\ \mu\text{m}$, $w=10\ \mu\text{m}$. (b) the structural parameters of the SLR-C unit cell. $P=125\ \mu\text{m}$, $a=120\ \mu\text{m}$, $R=30\ \mu\text{m}$, $P_2=100\ \mu\text{m}$. (c) and (d) are transmission spectra of individual sample with different structural for single layer and two layer

As shown in Figure 1, a single band absorber is designed which is composed of only one ring. A 500-nm thickness of gold was deposited on a 50-m-thick polyimide substrate. The radius of the ring is $150\ \mu\text{m}$. The size of the square unit is $170\ \mu\text{m} \times 170\ \mu\text{m}$. All the simulation of the metamaterial unit is optimized and obtained with CST Microwave Studio, choosing periodic boundary conditions along the x-axis and y-axis directions and open-add-space condition along the z-axis. From Figure 2(a), we can find that the metamaterial with single ring produce a wide resonant band around the frequency of 0.22 THz and strong absorption peak of 98%. It can be found from the current distribution (Figure 2(b)) on the ring that the current symmetrically concentrates on the

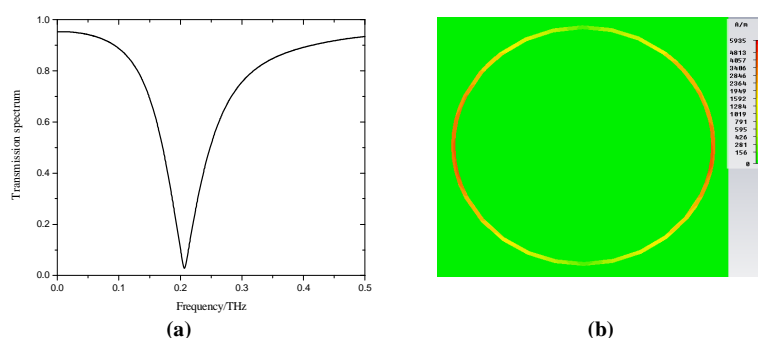


Figure 2. The simulated transmission spectra and surface current distribution of the proposed single resonant metamaterial absorber. (a) simulated transmission spectra of the proposed structure. (b) surface current distribution at 0.22 THz

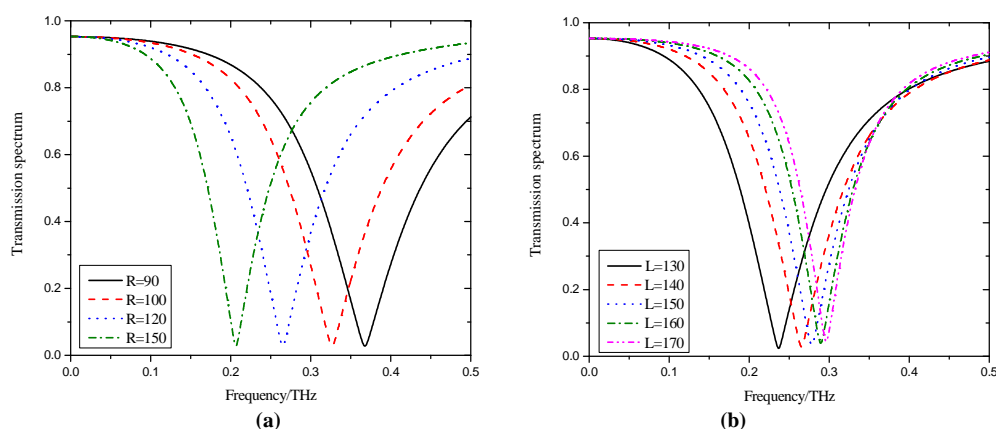


Figure 3. The simulated transmission spectra when sweeping R and L respectively. (a) R varies from $90\ \mu\text{m}$ to $150\ \mu\text{m}$. (b) L varies from $130\ \mu\text{m}$ to $170\ \mu\text{m}$ fixing R at $120\ \mu\text{m}$

left and right side of the ring, while the top and bottom of the ring have little current. It mainly depends on the polarization direction of the E field. The resonant frequency is determined by the semi-perimeter of the ring. From Figure 3(a), when the radius increases, the semi-perimeter of the ring becomes longer, the resonant frequency shifts to the low frequency (redshift). Similarly, when the radius decreases, it can be found that resonance frequency shifts to the high frequency (blueshift).

To understand the impact of the side length of the unit cell to the absorption peak, parameter sweep is performed. Figure 3 shows the simulated transmission spectra when sweeping L for the single ring arrays with radius $R=120\mu\text{m}$. From Figure 3(b), we can find that with L increasing, the resonance frequency will blueshift and the resonance bandwidth as same as the absorption peak become little. It is because that the mutual coupling among rings decreases with the length of L increasing. As the distance between adjacent two unit adds, effective dielectric constant of the absorber based on metamaterial is changed, which in turn changes the resonance frequency.

2. DESIGN OF DUAL RESONANT METAMATERIAL ABSORBER

As shown in Figure 4, two concentric rings are proposed to produce dual absorption bands. The radius of the big ring is as same as the ring mentioned above ($150\mu\text{m}$) and the radius of the small one is fixed at $100\mu\text{m}$. The simulate transmission characteristic shows that the structure can perform absorption peaks at two resonant frequencies 0.22 THz and 0.38 THz with the absorption about 97% and 96% . From Figure 5, at the frequency 0.22 THz , the current mainly flows through the big ring. Similarly, the current is mainly distributed in the small ring at 0.38 THz . The big ring and the small ring have little influence each other, which shows the two rings keep well-separated.

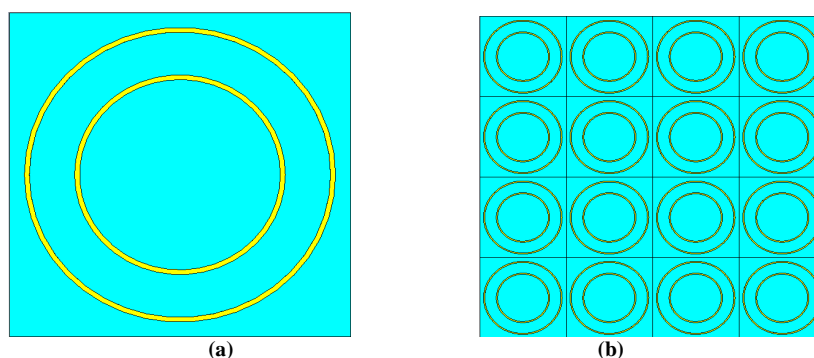


Figure 4. The dual-resonant THz metamaterial. (a) the dual-resonant unit cell. (b) a portion of the proposed metamaterial.

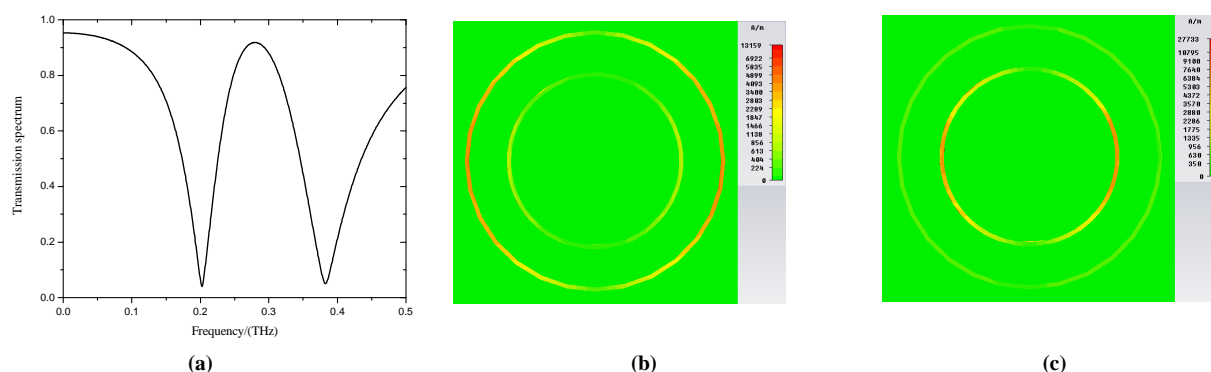


Figure 5. The simulated transmission spectra and surface current distribution of the proposed dual resonant metamaterial absorber. (a) simulated transmission spectra of the proposed structure. (b) surface current distribution at 0.22 THz . (c) surface current distribution at 0.38 THz

3. DESIGN OF TRIPLE RESONANT METAMATERIAL ABSORBER

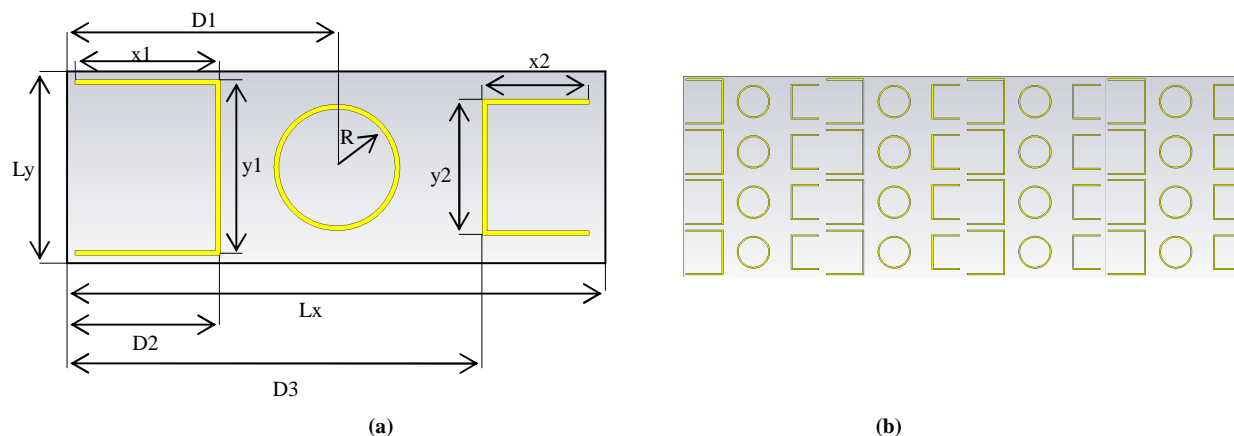


Fig. 6. (Color online) The structure of the triple-resonant THz metamaterial absorber. (a) geometries of triple-resonant unit cell. (b) a portion of the TRTA

The designed asymmetric triple-resonant THz absorber is shown in Fig. 6. Fig. 6(a) shows the geometries of a triple-resonant unit cell. Fig. 6(b) shows a portion of the unlimited cyclical array of the unit. The resonant unit consists of one ring and two split rings. Each resonator produce an absorption peak to the THz wave. The dimensions of a resonant unit are as follows: $L_x=560\ \mu\text{m}$, $L_y=200\ \mu\text{m}$, $D_1=280\ \mu\text{m}$, $D_2=160\ \mu\text{m}$, $D_3=430\ \mu\text{m}$, $x_1=150\ \mu\text{m}$, $x_2=110\ \mu\text{m}$, $y_1=180\ \mu\text{m}$, $y_2=140\ \mu\text{m}$, $S=5\ \mu\text{m}$, $R=65\ \mu\text{m}$.

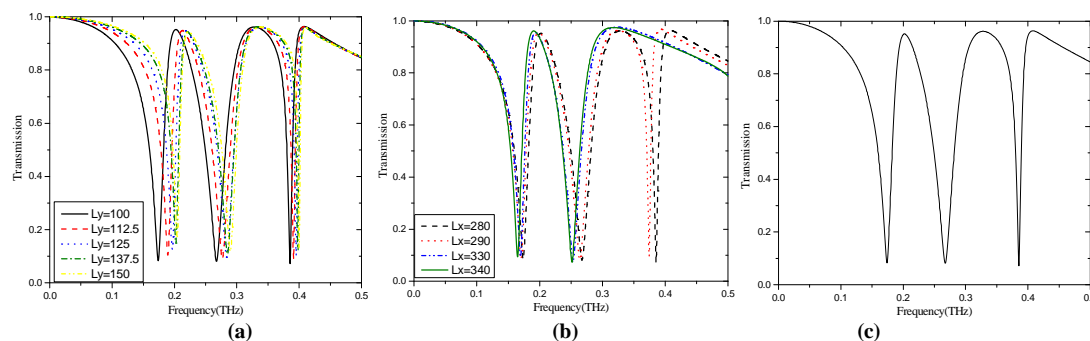


Figure 7. Simulated transmission characteristics of the proposed structure and The relationship of variation of Size of L_x and L_y and resonances of the TRTA. (a) Simulated transmission characteristics of the proposed structure. (b) Variation of L_x . (c) Variation of L_y

Figure 7 shows the simulated transmission characteristics of the proposed triple-resonant THz absorber applying CST. It shows that the proposed structure realizes triple resonant at 0.174 THz, 0.2675 THz and 0.3855 THz with absorption peaks strength 92.39%, 92.8% and 94.16%, respectively, which are produced by two split resonators and a ring. Because of coupling among adjacent unit cells, the size of L_x and L_y will influence resonant frequency and resonant-band width. As shown in Figure 7(b), when L_x increases, the three resonant frequency will decrease, and the highest resonant frequency at 0.3855 THz will disappear when L_x increase to 330 μm . On the other hand, as L_y increases, the three resonant frequency shift to high frequency and the absorption strength reduces simultaneously as shown in Figure 7(c).

Figure 8 show the surface current stimulated by the incident wave in the triple resonant structure. It can be found that the three resonant frequencies are caused by different resonant structure respectively. The surface current mainly concentrates on the left big split resonator near the lowest resonant frequency 0.174 THz, while the surface current of the other two resonators is weak. At the second resonant frequency 0.2675 THz, surface current mainly flows through the right small split resonator and it concentrates on the middle ring near the highest resonant frequency 0.3855 THz. It shows that the three resonators keep well-separated each other.

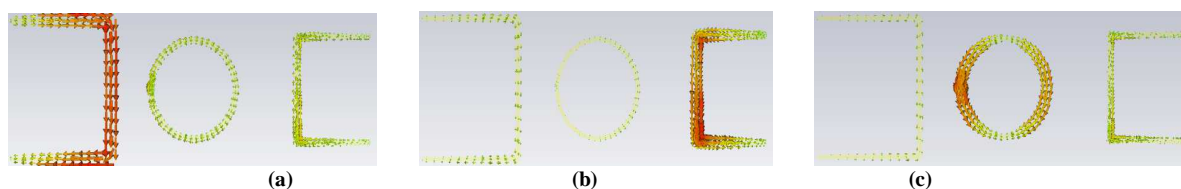


Figure 8. (Color online) The circular surface current distribution of designed TRTA near different resonant frequencies. (a) Near the lowest resonant frequency 0.174 THz. (b) Near the middle resonant frequency 0.2675 THz. (c) Near the highest resonant frequency 0.3855 THz

RESULTS AND DISCUSSION

1. SLOT IN DIFFERENT POSITIONS

To study the influence of the polarization direction of the incident wave to metamaterial resonance characteristics, we will compare the performance of the ring resonator to the conventional split ring resonator (SRR) designs. For better comparison, we choose same condition in the three design as 500-nm thickness of gold and 50- μm thickness of polyimide substrate. A radius $R=120\ \mu\text{m}$ of ring resonator and SRR (gap up), $R=50\ \mu\text{m}$ of SRR (gap left) and a lattice constant of $L_x=L_y=150\ \mu\text{m}$ would be chosen so that the resonance at a similar frequency of the four structures. Figure 9 shows simulations of the transmission spectra.

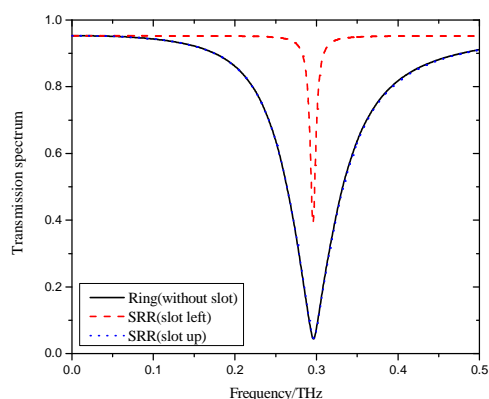


Figure 9. Simulated transmission through a ring resonator, and two split ring resonators

As is shown in Figure 9, the resonant frequency of ring resonator is 0.295 THz with a FWHM bandwidth of 122 GHz. And the one of the SRR (slot up) is exactly the same with the ring resonator both in resonant frequency and FWHM bandwidth. In other words, the slot in the top of the ring have little effects on the transmission characteristics of the THz wave. However, for SRR (slot right), the resonant frequency is 0.295 THz with a FWHM bandwidth only 9.5 GHz. Conventionally, the Q-factor, defined as $Q=f_r/\Delta f$ (the ratio between the resonance frequency f_r and the bandwidth Δf determined at the FWHM), is a measure of the photon life time in the resonator, and it is usually related to the sharpness of the resonance. The Q-factors of the ring resonator, SRR (slot up), SRR (slot right) and SCR are 2.4, 2.4, 31.11, respectively. The Q-factor of the SRR (slot right) is further higher than the ring resonator and SRR (slot up). For absorption peak, the ring and SRR (slot up) structure can achieve a high value of 97%, while the SRR (slot right) only have a absorption peak of 71.4%, which shows that the ring and SRR (slot up) structure perform better in absorption strength.

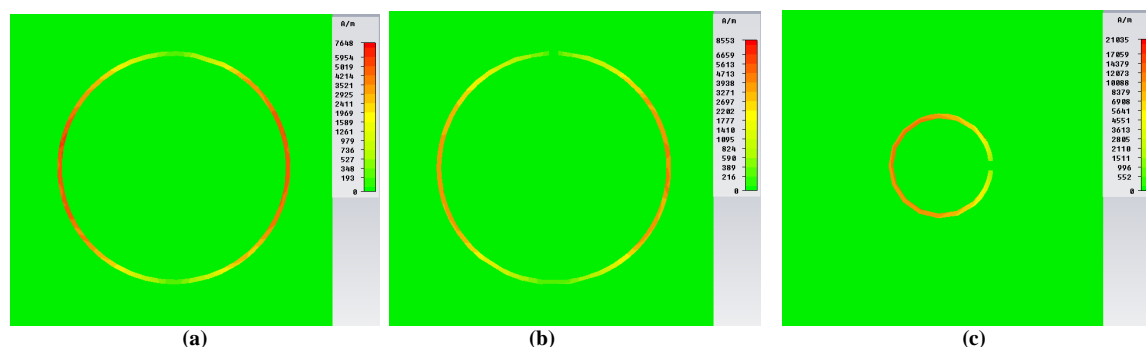


Figure 10. The surface current distribution of the proposed ring and SRR arrays. (a) surface current distribution on the ring. (b) surface current distribution on the SRR (slot up) at 0.295 THz. (c) surface current distribution on the SRR (slot right) at 0.295 THz

As shown in Figure 10(b), for SRR (slot up), same as ring resonance, the current direction of the left ring resonance is contrary to the current direction of the right ring resonance, and the split has little effect on the current distribution. But for SRR (slot right), the current direction is consistent throughout the whole resonance. So the electrical length of SRR (slot right) is longer than SRR (slot up). With same resonant frequency, the SRR (slot right) structure has more smaller radius and higher Q-factors than SRR (slot up). The ring resonance and SRR (slot up) structure have a bigger radius than the SRR (slot right). Thus the distance among adjacent resonant cells is smaller, which leads to stronger coupling and higher absorption peak.

2. DUAL LAYER RESONANT STRUCTURE

We study the effect of dual layer resonant structure on the THz wave transmission characteristics. The unit cell of the metamaterial is composed of two-layer metal circle plated on surface of the 50- μm polyimide substrate. The radius of the metal circle is 125 μm . The direction of electric field is perpendicular to the x coordinate and the direction of magnetic field is parallel to x coordinate. Fig. 11 shows the single layer unit cell and the transmission characteristic curve. Fig. 12 shows the single layer unit cell and transmission characteristic curve.

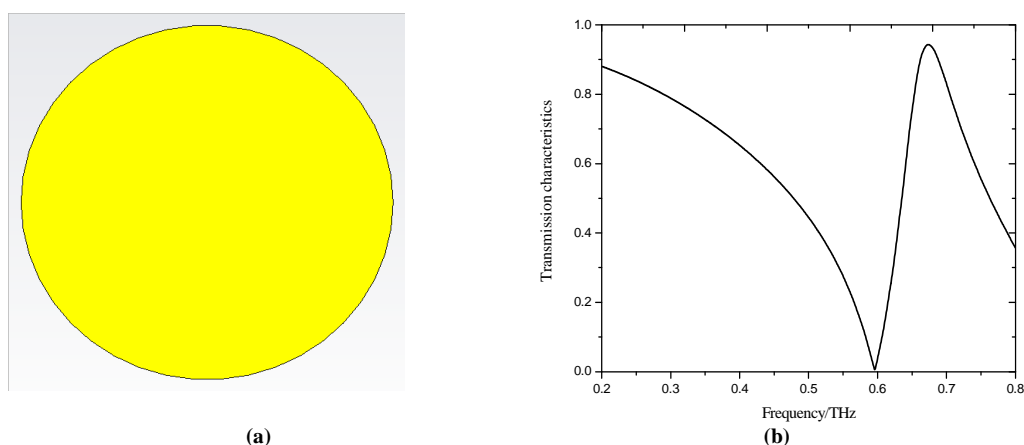


Figure 11. The unit cell of the single layer metamateria and the transmission characteristic curve

As show in Figure 11(b), the proposed single layer structure achieves strong absorption of 99.5% at 0.6 THz but has a slow falling edge in the bandstop. From Figure 12(b), the dual layer metamaterial realizes a wide absorption band from 0.4 THz to 0.71 THz (below 0.2 in the transmission curve) and fast rising and falling edge. Dual layer design enhances the metamaterial absorption strength to THz wave. The dual layer metamaterial with fast rising and falling edge may be useful in the THz filter applications.

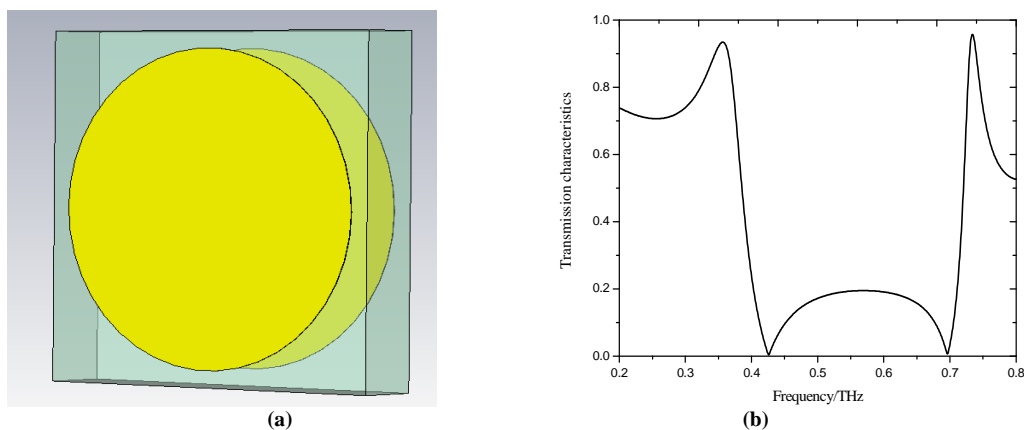


Figure 12. The unit cell of the dual layer metamateria and the transmission characteristic curve

CONCLUSION

In conclusion, we have designed three THz metamaterial absorber. The single band absorber achieves a wide resonant band around the frequency of 0.22 THz and strong absorption peak of 98%. The dual band absorber realizes two resonant frequency at 0.22 THz and 0.38 THz with the absorption about 97% and 96%. The asymmetric triple-resonant THz absorber have three distinct resonances near 0.174 THz, 0.2675 THz and 0.3855 THz with the

absorption peak strength of 92.39%, 92.8% and 94.16%. Our designed structures are uncomplicated, well-separated and strong-absorbed, which is beneficial for the design of multi-band terahertz devices.

REFERENCES

- [1] D. Schurig; J. J. Mock; B. J. Justice; S. A. Cummer; J. B. Pendry; A. F. Starr and D. R. Smith, *Science.*, **2006**, 314(5801), 977-980.
- [2] S. A. Ramakrishna, *Rep. Prog. Phys.*, **2005**, 68(2), 449-521.
- [3] J. B. Pendry, *Phys. Rev. Lett.*, **2000**, 85(18), 3966-3969.
- [4] Shraddha Shukla, Anupama Kashyap and Anil Kashyap, *Academic J. Cancer Res.*, **2013**, 5(9), 142-145
- [5] Lingfeng LI; Changhui XU; Yunxia Chen and Feng Xiao, *Academic J. Cancer Res.*, **2013**, 5(9), 555-562
- [6] D. R. Smith and N. Kroll, *Phys. Rev. Lett.*, **2000**, 85(14), 2933-2936.
- [7] Jiafu Wang, Shabo Qu, Yiming Yang et al., *Appl. Phys. Lett.*, **2009**, 95, 014105-014105-3.
- [8] X.C. Zhang; Y. Jin, T. D. Hewitt T. et al., *Appl. Phys. Lett.*, **1993**, 62, 2003-2005.
- [9] B. Heshmat; H. Pahlevaninezhad and T. E. Darcie, *IEEE Photonics Journal.*, **2012**, 4, 970-985.
- [10] Li Jiu-sheng, Liu Jian-jun, *Microwave And Optical Technology Letters.*, **2011**, 53(2), 267-278.
- [11] Fabio Alves, Brian Kearney, Dragoslav Grbovic et al., *Appl. Phys. Lett.*, **2012**, 100, 111104, 1-3.
- [12] Xiaopeng Shen, Yan Yang, Yuanzhang Zang et al., *Appl. Phys. Lett.*, **2012**, 101, 154102, 1-4.
- [13] Qi-Ye Wen, Huai-Wu Zhang, Yun-Song Xie et al., *Appl. Phys. Lett.*, **2009**, 95, 241111, 1-3.
- [14] Ya-Xin Zhang; Shen Qiao; Wanxia Huang et al., *Appl. Phys. Lett.*, **2011**, 99, 073111, 1-3.
- [15] Zhang-jing Wang, Shen-hui Guo, Jiang-jiang Li and Fei-ying Wang, *Academic J. Cancer Res.*, 2014, 6(4): 96-100
- [16] Jianguang Han, Jianqiang Gu, Xinchao Lu et al., *Optics Express.*, **2009**, 17, 16527.
- [17] Xiaoyu Zhang, Renbing Tan, ZhongXin Zheng et al, *J. Appl. Phys.*, **2013**, 113, 014504, 1-4.
- [18] Yi-Ju Chiang, Chan-Shan Yang, Yu-Hang Yang et al., *Appl. Phys. Lett.*, **2011**, 99, 191909, 1-3.
- [19] Dong Kwon Kim, D. S. Citrin, *IEEE journal of selected topics in quantum electronics.*, **2008**, 14(2). 416-420.